

# Light-induced structural changes and their correlation to metastable defect creation in intrinsic hydrogenated amorphous silicon films

Daxing Han, Jonathan Baugh, and Guozhen Yue

*Department of Physics and Astronomy, University of North Carolina at Chapel Hill, North Carolina 27599-3255*

Qi Wang

*National Renewable Energy Laboratory, 1617 Cole Blvd., Golden, Colorado 80401*

(Received 14 April 2000)

Device-quality intrinsic *a*-Si:H films were prepared by three methods, hot-wire (HW) chemical vapor deposition (CVD), and glow-discharge (GD) CVD with and without H dilution, and show varied light-induced metastable defect creation [Staebler-Wronski effect (SWE)]. We found the following: (a) In addition to the nonuniform H distribution, the *a*-Si network is inhomogeneous, and the film prepared by GD is more homogeneous than the HW film. (b) The light-induced increase of Si-H stretching absorption at  $\sim 2000\text{ cm}^{-1}$  is on the order of  $10^{-2}$  in all the films, and an additional decrease at  $\sim 2025\text{ cm}^{-1}$  is found in films with larger SWE. (c) The change of the compressive stress is on the order of  $10^{-4}$  of the initial value in the HW films, which is the same order of magnitude as in GD films. Both the initial stress and light-induced volume expansion decrease with decreasing Si-H concentration. No simple correlation between the light-induced structural changes and the conductivity changes was found in the HW *a*-Si:H films. We describe the light-induced structural changes in conjunction with the creation of metastable defects by a two-phase model.

## I. INTRODUCTION

Hydrogenated amorphous silicon (*a*-Si:H) is of great technological importance for solar cell and display applications, especially for light-weight, flexible substrates and large-area devices. Light-induced metastable defect creation in *a*-Si:H, the so-called Staebler-Wronski effect (SWE), has been the main problem limiting the application of this material.<sup>1</sup> Much progress has been made toward understanding and reducing the metastability.<sup>2-4</sup> There are two typical models to describe the kinetics of light-induced dangling-bond (DB) creation: weak-bond breaking due to carrier recombination,<sup>3</sup> and metastable DB creation by hydrogen collision.<sup>4</sup> Both models lead to the same defect creation rate equation, and the latter can explain the DB creation at low temperatures.<sup>4</sup> Whereas the weak-bond model describes the SWE as a local effect, the H collision model requires long-range H motion. These kinetic models<sup>3,4</sup> are based on the assumption of a uniform network with one type of recombination center; i.e., neutral dangling bonds ( $D^0$ ). In order to find the microscopic origin of the SWE, techniques have been developed to study light-induced structural changes in *a*-Si:H films.<sup>5,6</sup> Using the differential infrared absorption (DIR) technique, a light-induced reversible increase of  $\sim 1\%$  of the Si-H stretching mode at wave number  $2000\text{ cm}^{-1}$  was observed.<sup>5</sup> On the other hand, a light-induced expansion of 0.01% of the initial value was observed using the laser-optical cantilever-bending method (LOB).<sup>6</sup> The authors of both works<sup>5,6</sup> have shown that the light-induced structural changes obey the same stretched exponential rule as the dangling-bond defect creation that was characterized by degradation of photoconductivity (PC). Hence, the results imply that the metastable structural and conductivity (SWE) changes share the same microscopic origin. It is worth mentioning that the *a*-Si:H films were prepared by glow-discharge (GD) with a low H

chemical vapor deposition (CVD) dilution ratio of  $\text{SiH}_4:\text{H}_2=1:4$  and at substrate temperatures from 200 to  $250\text{ }^\circ\text{C}$  in both the DIR and LOB studies.<sup>5,6</sup>

One recent calculation suggested that a flipping of H to the Si back bond changes the oscillator strengths of Si-H vibrations.<sup>7</sup> The dipole moment of each flipped H can increase by a factor of 1.2–2. Therefore, a 0.01–0.1% H flip induces a  $10^{-4}$ – $10^{-3}$  increase in the  $2000\text{ cm}^{-1}$  absorption. Meanwhile, the distortions of the structure induced by H flips increase the strain of the network by about  $10^{-4}$ . This H flipping defect is suggested to occur in conjunction with the formation of metastable DB's, and the model predicts light-induced IR absorption and volume dilation on the same orders of magnitude as observed experimentally.<sup>5,6</sup>

Despite a great deal of progress made in understanding the metastability, materials with improved electronic stability have been made largely by technical means, e.g., by hot-wire (HW) chemical vapor deposition techniques<sup>8</sup> and by using hydrogen dilution in the conventional glow-discharge CVD.<sup>9-11</sup> For H-diluted *a*-Si:H, transmission electronic microscopy results show that the *a*-Si alloy is a heterogeneous mixture of an amorphous network and embedded more highly ordered regions. The volume fraction of the more highly ordered regions increases with increasing hydrogen dilution.<sup>9</sup> For device-quality HW *a*-Si:H, only 2–3 at. % H is needed, compared to 8–10 at. % in GD CVD samples. Furthermore, a NMR study suggests that most H atoms are highly clustered in relatively small volume fractions in HW films.<sup>12</sup> In the low-H-content HW films, it was found that the internal friction is much smaller than in GD films.<sup>13</sup> This further indicates that the HW *a*-Si:H network has better overall fourfold coordination. Therefore, improved structural ordering could be a key factor resulting in the improvement of electronic stability. In this work, we study light-induced structural changes in relation to the SWE behavior. Three

TABLE I. Sample preparation conditions and parameters for H microstructure studies.

Sample no.	Deposition method	Substrate temperature (°C)	Reaction gas	Growth rate (Å/s)	Film thickness (μm)	H content (at. %)
1	HW CVD	410	pure silane	8	~7	~1
2	GD CVD	200	13:1 H diluted	1	~4	8
3	GD CVD	200	pure silane	4	~5	12

types of device-quality *a*-Si:H films were chosen: HW films, and GD CVD *a*-Si:H made with and without H dilution. Concerning the SWE, the HW films made at  $T_{\text{fil}} = 1900^\circ\text{C}$  and  $T_s$  from 360 to 400 °C are more stable than the low-H-diluted GD *a*-Si:H; moreover, the non-H-diluted film is less stable than the H-diluted GD *a*-Si:H. This work aims to answer the following question: if a correlation exists between the light-induced structural changes and the SWE,<sup>5,6</sup> should the light-induced structural changes also be reduced in the HW *a*-Si:H films and enhanced in the non-H-diluted *a*-Si:H film? The experimental results yield insights into the microscopic origin of the SWE.

## II. SAMPLES AND EXPERIMENT

Device-quality intrinsic *a*-Si:H films were prepared by three typical techniques, i.e., by glow-discharge CVD without hydrogen dilution and with low hydrogen dilution at Solarex and by hot-wire CVD techniques at National Renewable Energy Laboratory (NREL). The films were examined by x-ray, Raman, and photoluminescence techniques, and found to be fully amorphous, without microcrystallinity. The defect density was  $\leq 10^{16}\text{cm}^{-3}$  for all the samples studied. The measurements of light-induced structural changes were carried out with the help of investigators using the DIR and LOB techniques in their laboratories. Experimental details can be found elsewhere.<sup>5,6</sup>

For the differential infrared absorption measurements, *a*-Si:H films were deposited on intrinsic crystalline Si wafers ( $r > 100\text{W cm}$ ). In order to eliminate interference effects, the silicon wafers were single-side polished and the *a*-Si:H film was deposited on the rough side. The sample preparation conditions, thickness, and hydrogen content are listed in Table I. Differential infrared absorption spectra were measured with a home-made spectrometer. The sensitivity of the DIR instrument is about two orders of magnitude higher than for commercially available IR instruments. This allows detection of subtle changes of the IR absorption in a 5-μm-thick *a*-Si:H film. The DIR measurements focused on the wave-number range from 1800 to 2300  $\text{cm}^{-1}$ , where the characteristic peak of the Si-H stretching vibration mode is located. State A was reached by annealing the initial state of the sample at 160 °C in vacuum to remove surface absorption and metastable defects. The measurements were then carried out after step-by-step light soaking with 90  $\text{mW/cm}^2$  white light with an infrared cutoff filter. Finally, the sample was annealed at 200 °C in vacuum for 1 h to check the reversibility.

For the laser-optical cantilever-bending studies, 1.0-μm-thick *a*-Si:H films were deposited on 100-μm-thick  $2 \times 20\text{mm}^2$  flat quartz substrates by hot-wire CVD. The films

were also deposited on 7059 glass and crystalline-silicon substrates for conductivity and H content measurements. The sample preparation conditions, thickness, and hydrogen content are listed in Table II. The film-quartz system bends due to both the film volume stress during the growth process and the difference in the thermal expansion coefficients of the film and the substrate. In the LOB measurements, the detection limit was  $5 \times 10^{-6}$  rad, which corresponds to a small displacement at the edge of the sample,  $\sim 70$  Å. This allows us to detect  $\sim 0.01$  MPa of stress in the *a*-Si:H films. One piece of the quartz substrate without *a*-Si:H film was used as the zero-bending reference. The samples were light soaked using 300  $\text{mW/cm}^2$  white light, and were then annealed at 200 °C for 1 h. Both the light soaking and annealing were done *in situ*. We note that the light-soaking source was 3.3 times stronger than that used in the DIR studies. The PC degradation and conductivity activation energy measurements were carried out for the films deposited on 7059 glass.

Three films, identical to samples 1, 2, and 3 above, were prepared for NMR studies. The <sup>1</sup>H NMR spectra were measured using a simple one-pulse technique and recording the subsequent free-induction decays. The home-built <sup>1</sup>H NMR probe was thoroughly cleaned and found to have a low relative <sup>1</sup>H background signal. The NMR experimental details can be found elsewhere.<sup>12</sup>

## III. RESULTS

### A. H microstructure measured by IR and NMR

It is generally believed that the metastability phenomenon is related to hydrogen in *a*-Si:H.<sup>1-4</sup> In order to compare the H microstructure in the three device-quality *a*-Si:H films made by different techniques, the H configuration and its distribution were measured by IR absorption and NMR spectroscopies, respectively. Figure 1(a) shows the IR absorption spectra for samples 1, 2, and 3 listed in Table I measured with a commercial IR instrument. The top curve for sample 1

TABLE II. HW film preparation conditions and parameters for LOB studies.

Sample no.	Substrate temperature (°C)	Filament current (Å)	Growth rate (Å/s)	Film thickness (μm)	H content (at. %)
TH287	280	14	7.5	~1	7
TH286	320	14	8.0	~1	5
TH185	360	15	8.0	~1	3
TH186	400	15	8.3	~1	2
TH188	440	15	11	~1	<1

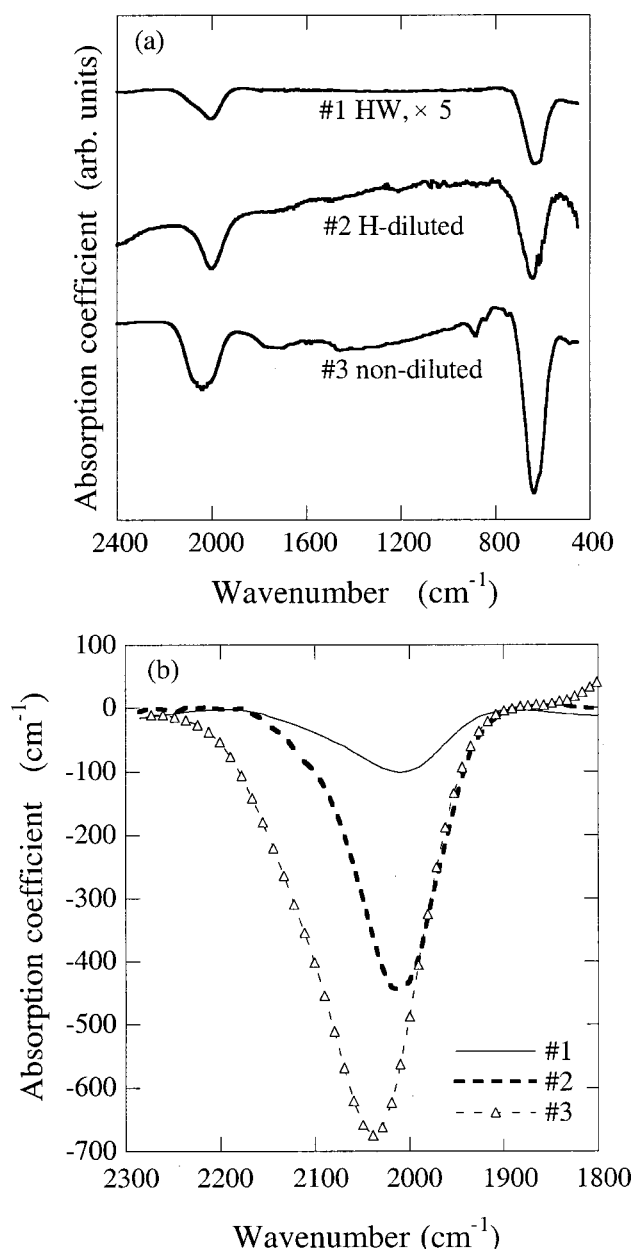


FIG. 1. (a) IR spectra and (b) the normalized stretching mode for the HW (sample 1), the H-diluted GD (sample 2), and the non-H-diluted GD (sample 3), *a*-Si:H films.

(HW film) was enlarged five times. The H content deduced from the Si-H bending mode at  $630\text{ cm}^{-1}$  is 1, 8, and 12 at. % for samples 1, 2, and 3, respectively. In Fig. 1(a) only the  $630\text{ cm}^{-1}$  bending and the  $2000\text{ cm}^{-1}$  stretching modes of the Si-H bond can be resolved for samples 1 and 2. For the non-H-diluted film, sample 3, a small  $890\text{ cm}^{-1}$  absorption peak from the bending mode of the Si-H<sub>2</sub> configuration can be seen. Meanwhile, the broad absorption peak centered at  $2040\text{ cm}^{-1}$  could be a combination of the stretching-mode absorptions of Si-H and Si-H<sub>2</sub>. In Fig. 1(b), we show the absorption coefficient of the stretching mode measured with the home-made spectrometer. The data agree well with the IR spectra in Fig. 1(a). The broad peak of sample 3 can be deconvoluted into two Gaussian functions peaked at  $\sim 2010$  and  $2080\text{ cm}^{-1}$ , related to the Si-H and Si-H<sub>2</sub> stretching modes, respectively. However, one cannot distinguish by IR

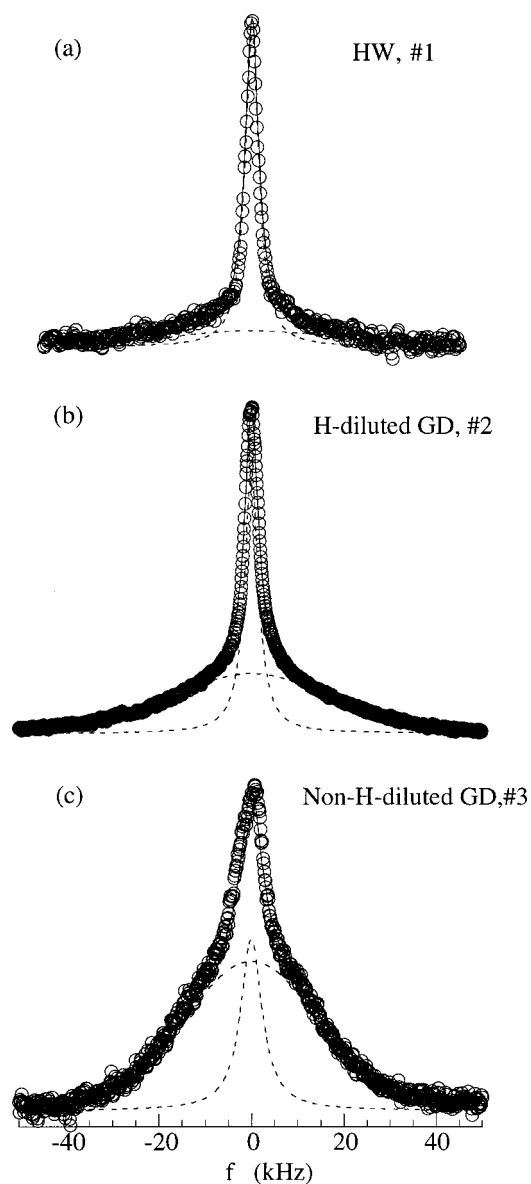


FIG. 2. NMR spectra for the HW (sample 1), the H-diluted GD (sample 2), and the non-H-diluted GD (sample 3), *a*-Si:H films.

spectroscopy whether the Si-H bonds are clustered or isolated. The H spatial distribution was clarified by NMR measurements, as shown in Fig. 2.

NMR spectra for films prepared in the same conditions as those in Fig. 1 are shown in Fig. 2. Figures 2(a), 2(b), and 2(c) correspond to samples 1, 2, and 3, respectively. The spectra are fitted well by a Gaussian function for the broad peak and a Lorentzian function for the narrow peak, which represent clustered and isolated H environments, respectively. The area under each curve is proportional to the total number of <sup>1</sup>H spins contributing to the signal producing the curve. Thus, the ratio of the areas of the narrow and broad peaks gives the relative amount of H in the isolated versus the clustered phase. The linewidths and intensity ratios of narrow and broad components are listed in Table III.<sup>14</sup> Despite the large difference in H content of the HW and H-diluted GD films, the ratio of isolated to clustered H is nearly the same in samples 1 and 2. On the other hand, the nondiluted film sample 3 contains much more clustered H.

TABLE III. H distribution parameters from NMR spectrum.

Sample no.	Broad linewidth (kHz)	H-H separation in clustered phase (Å)	Narrow linewidth (kHz)	H-H separation in dilute phase (Å)	Ratio narrow: broad	Dilute H absent volume fraction
1	45	1.7	3.0	9	31:69	80%
2	35	1.9	3.9	7	34:66	22%
3	40	1.8	4.0	7	15:85	25%

Furthermore, the linewidth of the broad peak is a measure of the average compactness of the clusters; i.e., a larger width means a smaller average nearest-neighbor distance. The broad line of the HW sample 1 has the largest width,  $\sim 45$  kHz, compared to  $\sim 37$  kHz for the two GD samples 2 and 3. This indicates that the HW film has the most tightly compacted H clusters.<sup>12</sup> The narrow lines are about 3–4 kHz in all the samples. The H-H nearest-neighbor separations for both the clustered and the isolated phases are also given in Table III. Using the intrinsic dipolar broadening of the narrow peak obtained by the NMR technique of hole burning, as well as the H content, the volume fraction of the film containing isolated H can be estimated, assuming a random distribution of spins. The clustered-H-containing volume fraction is small compared to that of isolated H, so only the isolated H absent volume fraction is given in Table III. Interestingly, we found that a 20–80% volume fraction contains almost no isolated H in all the samples. This implies that there is an inhomogeneity of the backbone amorphous silicon network, in addition to the inhomogeneity of the H distribution. More interestingly, the HW sample 1 shows the largest volume fraction (80%) that is H poor. Therefore, in the sense of *a*-Si:H network homogeneity, the GD is better than the HW film. However, we have found that the HW film's H distribution can be made more homogenous if the deposition conditions are optimized.<sup>15</sup> In such a case, the NMR spectra show a higher percentage of H ( $\sim 45\%$ ) in the isolated phase.

The above IR and NMR results show that, despite the large difference in H content in the H-diluted GD and the HW samples, the hydrogen configurations and distribution are qualitatively similar, i.e., there is a predominance of Si-H bonds and more H in the isolated phase. Furthermore, the tightly compacted clusters and the large H-poor volume fraction of  $\sim 80\%$  in the HW film indicate improved structural ordering, but also a large structural inhomogeneity of the HW film. In contrast, the non-H-diluted sample contains Si-H<sub>2</sub> and shows more clustered Si-H as well. The next relevant question is, how does the H microstructure change upon light soaking in these three films? If there is a simple correlation between the light-induced increase of Si-H absorption and the SWE,<sup>5</sup> the DIR signal should be largest in the nondiluted GD sample 3, and smaller in the HW sample 1 compared to the H-diluted sample 2. The results are given in the next section.

### B. Light-induced changes of the Si-H absorption

State A was reached by 160°C annealing of the initial state of the sample in vacuum. The measurements were then

carried out after step-by-step light soaking with 90 mW/cm<sup>2</sup> white light for about 100 h. In Fig. 3, we show the saturated and intermediate curves of the DIR spectra; (a), (b), and (c) correspond to samples 1, 2, and 3, respectively. One can see in Figs. 3(a) and 3(b) that the saturated values show an increase of about 1% in the absorption near 2000 cm<sup>-1</sup> after light soaking for both the H-diluted and the HW films. This is quantitatively consistent with the results of Zhao *et al.*<sup>5</sup> for low-H-diluted GD *a*-Si:H films. For the nondiluted GD sample 3, the light-induced change is complex, including a

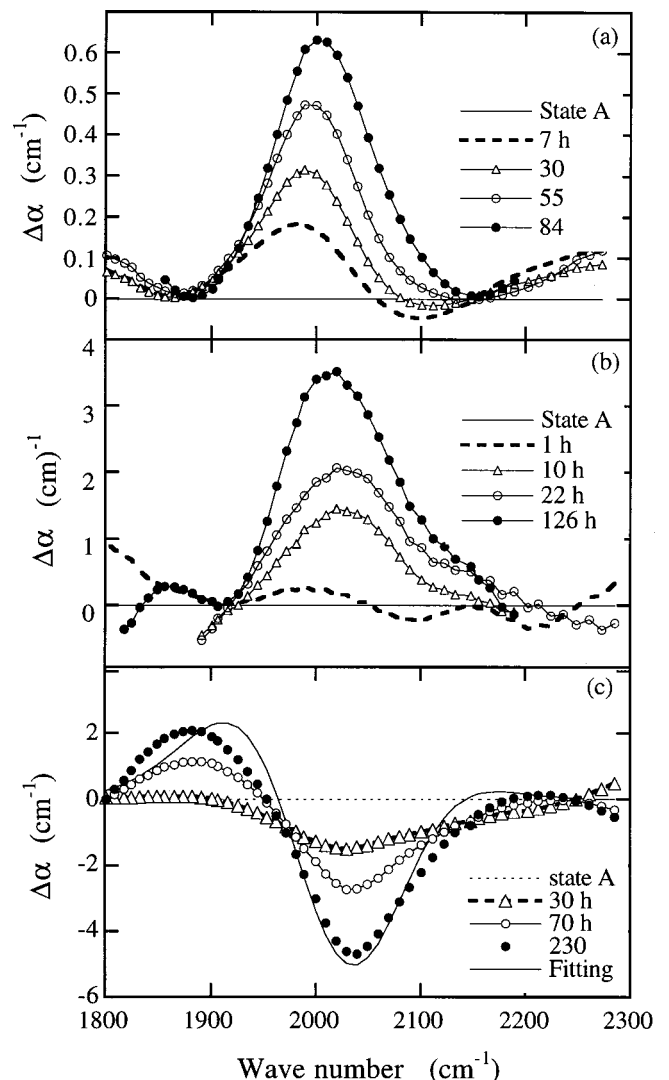


FIG. 3. Light-induced changes of IR absorption measured by DIR technique. (a), (b), and (c) correspond to samples 1, 2, and 3, respectively.

decrease near  $2040\text{ cm}^{-1}$  and an increase centered at  $1880\text{ cm}^{-1}$ . Indeed, there was only a decrease centered at  $2025\text{ cm}^{-1}$  after 30 h of light soaking. It is possible that there is a combination of the increase at  $\sim 2000\text{ cm}^{-1}$  due to metastable changes of Si-H and a decrease at a higher wave number due to metastable changes related to the Si-H<sub>2</sub> bonds. For instance, we obtain the fitting curve as the solid line shown in Fig. 3(c) by using two Gaussian functions, if we assume a 1% increase at  $\sim 2000\text{ cm}^{-1}$  and a 1.5% decrease at  $2025\text{ cm}^{-1}$ . Finally, the sample was annealed at  $200^\circ\text{C}$  in a vacuum for 1 h to remove the photoinduced changes. We observed an 80–90% recovery of the DIR spectrum for all samples. The lack of full recovery might be due to inhomogeneity of the film.

It was expected that the DIR increase at  $\sim 2000\text{ cm}^{-1}$  might be less in the HW than in the GD film. It was somewhat surprising that the DIR data show the same order-of-magnitude metastable increase at  $\sim 2000\text{ cm}^{-1}$  occurring in these three types of films. It is clear that there are light-induced IR absorption changes in these three films but the correlation with the SWE is not simple. The non-H-diluted GD film shows an additional decrease of the DIR signal at higher wave number. To further study how the metastable structural changes are correlated to the electronic stability, we show another type of light-induced structural metastability in the next section.

### C. Initial and light-induced stress in HW *a*-Si:H

Using a sensitive bending technique, a subtle increase of film expansion was found in GD *a*-Si:H films upon light soaking, and the kinetics of the light-induced structural change was identical to the kinetics of the SWE.<sup>6</sup> We performed the same measurements at the same laboratory on a group of HW *a*-Si:H films that are listed in Table II. Figure 4(a) shows the initial stress of the HW *a*-Si:H films as a function of both the substrate temperature  $T_s$  and the hydrogen content. The H content was deduced from the IR absorption spectrum. In Fig. 4(a), it is seen that the maximum initial compressive stress  $\sim 425\text{ MPa}$  corresponds to a relatively low deposition temperature  $T_s = 280^\circ\text{C}$  and high hydrogen content  $\sim 8\text{ at.}\%$ . As the deposition temperature increases, both the hydrogen content and the compressive stress decrease. The minimum compression of  $\sim 74\text{ MPa}$  occurs at a high deposition temperature of  $T_s = 440^\circ\text{C}$  and low hydrogen content of  $\leq 1\text{ at.}\%$ . This indicates that the higher the concentration of Si-H bonds, the higher the compression of the film, since we know that Si-H bonding is the dominant H configuration in the film. Figure 4(b) shows the photoinduced changes of the stress after  $300\text{ mW/cm}^2$  light soaking for 3 h in the same group of hot-wire *a*-Si:H samples. As in GD films,<sup>6</sup> the saturated light-induced expansion is on the same order of  $10^{-4}$  of the initial stress, and the light-induced expansion decreases with hydrogen content in the same manner as does the initial compression. The light-induced volume expansion was reversed by thermal annealing at  $200^\circ\text{C}$  for 1 h. Again, we did not see the expected results of less light-induced stress in HW *a*-Si:H than in GD CVD films; however, we did see that both the initial compression and the light-induced volume expansion are proportional to the Si-H bond concentration.

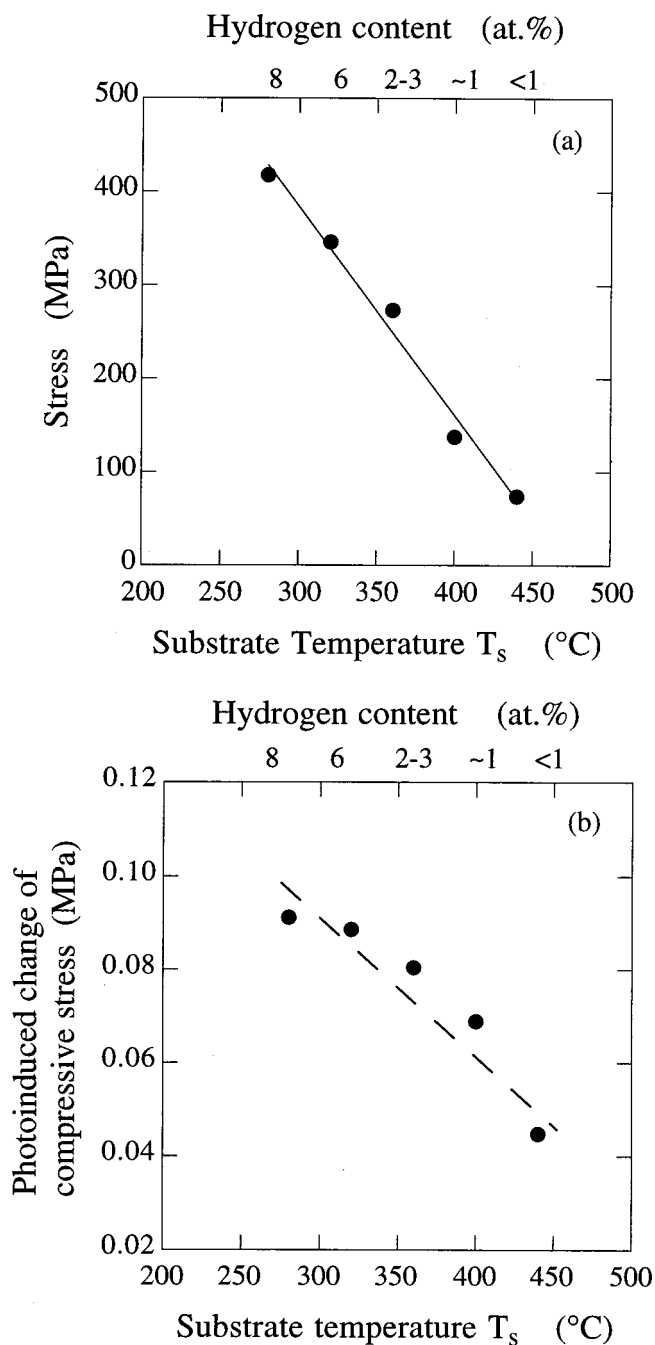


FIG. 4. (a) Initial compressive stress and (b) photoinduced changes of the stress after  $300\text{ mW/cm}^2$  light soaking for 3 h, as a function of substrate temperature and H content in a group of HW *a*-Si:H samples.

### D. Photoconductivity degradation and metastable defects in HW *a*-Si:H

In order to study the correlation of the film stress with the SWE in HW films, the photoinduced changes in both photo- and dark conductivities were measured for the same group of films investigated in the stress studies. The same light source for light soaking was used for the PC measurements. In Fig. 5 we show the PC decay as a function of light-soaking time. We can see that up to 15 h of light soaking with  $300\text{ mW/cm}^2$  white light causes the PC to decrease by about one order of magnitude for the films deposited at  $T_s = 280$  and  $320^\circ\text{C}$ , but a smaller decrease occurs for the films deposited

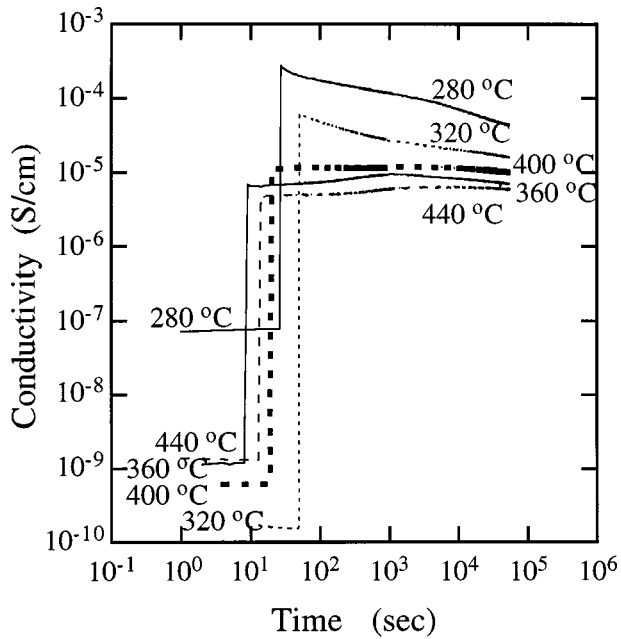


FIG. 5. Photoconductivity as a function of light-soaking time for the same HW samples as in Fig. 4.

at  $T_s \geq 360^\circ\text{C}$ . We note that some increases in PC can be seen over some time segments in samples deposited at 360 and 440 °C. Meanwhile, the temperature dependence of the dark conductivity was measured from room temperature up to 150 °C before and after light soaking. The position of the Fermi level deduced from the thermal activation energy of the conductivity is shown in Fig. 6. Comparing the results in Figs. 5 and 6, one finds that when the Fermi level moves down appreciably (from 0.60 to 0.83 eV and from 0.82 to 0.90 eV below the conduction band edge for the films deposited at  $T_s = 280$  and 320 °C, respectively) the PC decreases by a factor of 10; otherwise, the PC degradation effect is

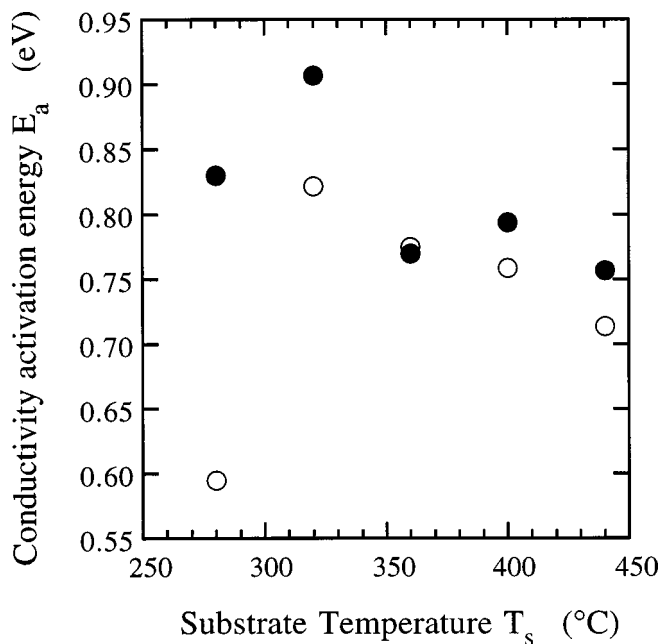


FIG. 6. Conductivity activation energy before (○) and after (●) light soaking for the same samples as in Fig. 4.

very small (in the films deposited at  $T_s \geq 360^\circ\text{C}$ ). Reasonably, if the metastable defect are created near the midgap, the Fermi level moves downward and the PC decreases upon light soaking. When fewer defects are created in the midgap ( $T_s \geq 360^\circ\text{C}$ ), neither the Fermi level nor the PC changes much. Nevertheless, none of the PC degradation curves obey the stretched-exponential law described by the existing models.<sup>3,4</sup> We noticed that typical values of the activation energy in HW films are not only larger than that in GD films ( $\sim 0.6$  and 0.75 eV at states A and B, respectively), but also nonreproducible during light-soaking–annealing cycles. In many cases, the activation energy is 0.9–1.0 eV in state A,<sup>16</sup> i.e., the Fermi level is located at or below midgap. The Fermi level then either moves upward or does not change upon light soaking. After annealing a second time, the activation energies are smaller than that measured in state A, about 0.7–0.8 eV.

One may argue that the defect density of states DOS is a better characterization of the electronic stability. To deduce the defect density of states, the subband absorption was measured by photothermal deflection spectroscopy (PDS) for the same group of HW films. We plot the results of PDS before light soaking in Fig. 7(a). We found that the subband gap absorption  $\alpha_{\text{ex}}$  is one to two orders of magnitude higher than that in device-quality films. Unexpectedly, the 360 °C film shows the highest subband gap absorption, which could correspond to a defect density  $\geq 10^{18}/\text{cm}^3$  deduced from the relation  $N_d = 7.9 \times 10^{15} \int \alpha_{\text{ex}} dE$ .<sup>17</sup> From our previous studies by both the constant photocurrent method and electron spin resonance, we know the defect density is less than  $10^{16}/\text{cm}^3$  in the film deposited at 360 °C. A possible reason for this discrepancy could be the high sensitivity of the PDS technique to surface roughness. Accordingly, we examined the film surface morphology by atomic force microscopy (AFM), and plot both the PDS and AFM results as a function of film deposition temperature in Fig. 7(b). The AFM result from a GD sample is also indicated. The surface roughness was defined by an average in a scanning area of  $1 \times 1 \mu\text{m}^2$ . A typical value of surface roughness for GD *a*-Si:H is 2–3 nm. On the other hand, we found that the roughness of these HW films was in the range of 5–19 nm. Figure 7(b) shows that there is clearly a correlation between the PDS and the AFM data, and hence the subband gap absorption signal from PDS is most likely due to surface roughness and not the bulk defect density for the HW *a*-Si:H films. The detailed explanation for the high PDS value remains unclear. Because of the high value introduced by the surface roughness, after light soaking there were no visible changes of the subband absorption in the PDS data.

The defect density  $N_d$  deduced from subband gap absorption by using the constant photocurrent method in connection with the transmission spectrum is a more reliable way to characterize metastable defect creation. All the transitions from deep states to transport level in the bulk material will contribute to the subband gap absorption.<sup>18</sup> We show the results from a group of HW films that were deposited on 7059 glass substrates using the same CVD system at the same substrate temperature series but all with filament current of 14 A. Film properties such as the H content, the initial photosensitivity, and the light-induced changes of the PC for each sample were similar to those listed in Table II.

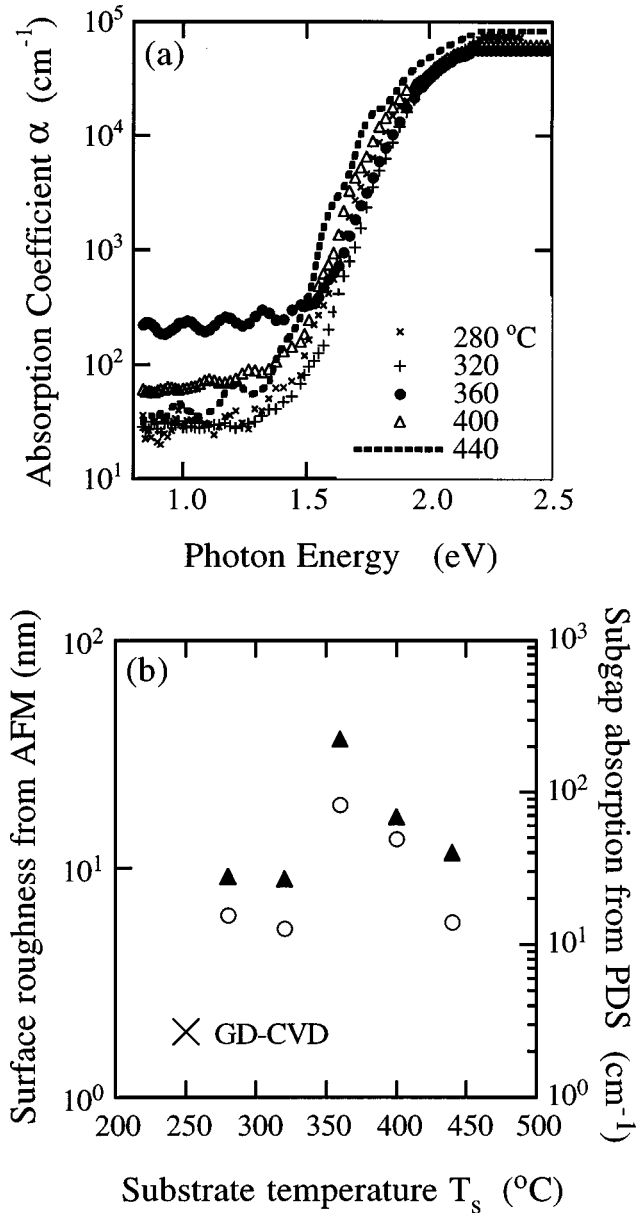


FIG. 7. (a) Subband gap absorption and the absorption edge measured by PDS, and (b) correlation of PDS (solid triangles) with AFM (open circles) data, showing that the subgap absorption signal is due to surface roughness for the same HW *a*-Si:H films as in Fig. 4. An AFM data point from a GD CVD film is also shown (x).

However, the PC degradation kinetics are slightly different. The details are given elsewhere.<sup>16</sup> In Fig. 8, we show the density of metastable defects  $\Delta N_d$  deduced from subgap absorption in comparison with that obtained from the PC results. The densities of metastable defects deduced from the PC and subband gap absorption are slightly different for most films; the light-induced defect density is about  $(1-2) \times 10^{16} \text{ cm}^{-3}$  in most films. The largest difference was found for the film deposited at 360 °C, in which the metastable defect density deduced from PC data was a factor of 6 larger than that from subgap absorption.

Comparing the light-induced volume expansion and the light-induced PC degradation as well as the defect creation, we found that, first, the better electronic stability of the HW *a*-Si:H does not result in a smaller light-induced volume ex-

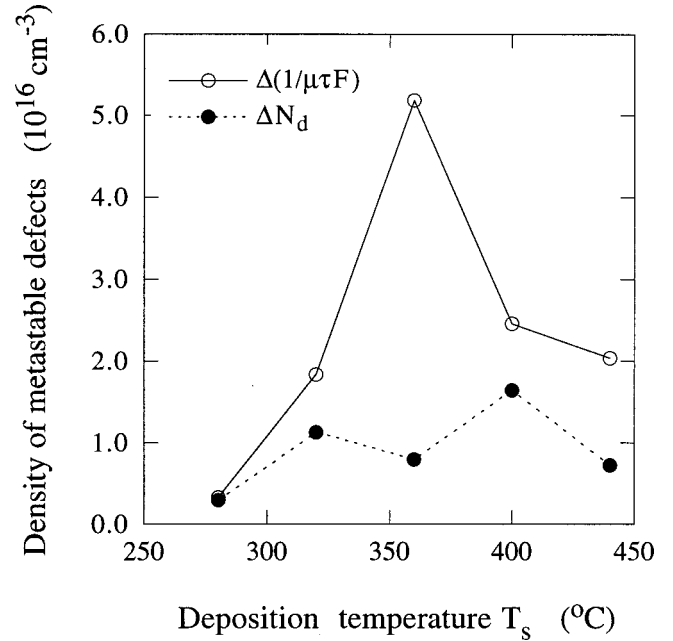


FIG. 8. The density of metastable defects  $\Delta N_d$  deduced from subgap absorption in comparison with that from the PC results for HW films deposited at substrate temperatures of 280, 320, 360, 400, and 440 °C with filament current 14 A.

pansion; secondly, in this group of HW films the light-induced volume expansion decreases when the film deposition temperature increases as shown in Fig. 4 (b). In contrast, the light-induced photodegradation of electronic properties such as the changes of PC, Fermi-level position, and defect DOS do not monotonically decrease as  $T_s$  increases, as shown in Figs. 5, 6, and 8.

#### IV. SUMMARY AND DISCUSSION

The hydrogen content and microstructure and their light-induced metastable changes were studied by IR, DIR, and NMR in device-quality *a*-Si:H samples that were prepared by hot-wire and glow-discharge CVD with and without H dilution. Despite the large difference in H content between the HW and H-diluted GD samples, 1 and 8 at. %, the H bonding configuration, its distribution, and the light-induced increase of IR absorption are qualitatively the same, i.e., a predominance of Si-H bonds,  $\sim \frac{1}{3}$  of the H in the isolated phase, and an IR absorption increase  $\sim 1\%$  near  $2000 \text{ cm}^{-1}$  upon  $90 \text{ mW/cm}^2$  light soaking for about 100 h. In contrast, the non-H-diluted sample with 15 at. % hydrogen contains Si-H<sub>2</sub> bonds in addition to Si-H bonds,  $\sim 85\%$  H is clustered, and a combination of increase and decrease of the DIR signal is observed. In agreement with previous studies,<sup>19</sup> we find that the Si-H bond configuration and an isolated distribution of Si-H are preferred for more stable materials, such as the H-diluted GD and HW films. The additional metastability is related to the H cluster and/or Si-H<sub>2</sub> bonds in the nondiluted GD film, in which a metastable decrease in absorption at  $\sim 2025 \text{ cm}^{-1}$  was found. However, both the mechanism that causes the decrease at  $\sim 2025 \text{ cm}^{-1}$  and how this relates to DB creation remain unclear.

Interestingly, the NMR results indicate that a 20–80 % volume fraction contains almost no H in all the samples. This

implies that there is an inhomogeneity of the backbone amorphous silicon network, in addition to the inhomogeneity of the H distribution.  $\sim 0.3$  at. % isolated H atoms are distributed in only  $\sim 20\%$  volume fraction in the HW film.  $\sim 2$ – $3$  at. % isolated H atoms are distributed in the majority of the volume (80%) in the GD films. The overall picture is that GD produces a more homogeneous *a*-Si:H network. The AFM results also indicate a better homogeneity of the GD than the HW film. However, the tightly compacted clusters and the large H-poor volume fractions of  $\sim 80\%$  in the HW films indicate improved structural ordering that could contribute to the improvement of electronic stability of the HW films.

Initial and photoinduced stress were studied in a group of hot-wire *a*-Si:H films deposited in a wide temperature range, from 280 to 440 °C. We observed a photoinduced increase of the compressive stress, that is, a volume expansion on the order of  $10^{-4}$  of the initial value. The change is of the same order of magnitude as that observed in GD films.<sup>6</sup> We found that both the initial compression and the light-induced volume expansion decrease monotonically with decreasing Si-H bond concentration in the HW films. This indicates that the Si-H bond contributes compressive stress to the Si network, and that the light-induced volume expansion is also related to the Si-H bond.

The densities of metastable defects deduced from the PC and the subband gap absorption show a slight difference for most HW films. The largest difference was found for the film deposited at 360 °C, in which AFM [Fig. 7(b)] shows the highest inhomogeneity. The light-induced defect density was of the order of  $10^{16}$  cm<sup>-3</sup>. No simple correlation between the SWE and the light-induced expansion was found in HW films, and none of the PC degradation curves obeyed a stretched-exponential rule.

Many experimental results have shown that PC degradation cannot be explained by the bimolecular recombination model,<sup>3</sup> in which the PC is inversely proportional to the density of neutral dangling bonds ( $D^0$ ). However, two or three types of recombination centers, such as neutral and charged DB's, can explain the experimental results.<sup>10,11,16,18,20,21</sup> It is known that the conductivity in intrinsic *a*-Si:H is dominated by mobile electrons. Therefore, the lack of agreement between the PC degradation and metastable defect creation can be understood if the film contains charged defects. For instance, if positively charged  $D^+$  are converted into neutral  $D^0$  (or  $D^0 \rightarrow D^-$ ) upon light soaking, the capture cross section for electrons will decrease, and consequently the PC will increase. For instance, the capture rate for electrons is  $\sim 10^{-10}$  and  $10^{-7}$  cm<sup>3</sup>/s for  $D^0$  and  $D^+$ , respectively,<sup>20</sup> which could result in electron lifetimes differing by a factor of  $10^3$ . If this event parallels the increase of the  $D^0$  defect density, the resultant PC could be stable or even increase upon light soaking. Charged defects are more likely to exist in an inhomogeneous film in which potential fluctuations are strong.<sup>22</sup> The large value of the activation energy may be due to the existence of charged defects.<sup>16</sup> The nonreproducible activation energy may indicate that the conversion or creation of charged defects is not completely reversible during light-soaking–annealing cycles. More research is needed to clarify what kind of charged defects there are and how they are converted in the light-soaking and annealing processes.

Based on our experimental results, we conclude that the amorphous silicon network is not a near-ideal continuous random network, but is rather an inhomogeneous network. One possible picture is that the film contains less ordered regions connecting more ordered domains, i.e., a two-amorphous-phase model in the simplest picture. Specifically, the interfacial regions between the phases are likely to be highly disordered and to contain clusters of H occupying shallow Si-H levels. The more ordered phase contains almost no H at all (the H-absent region found by NMR). Based on experimental observations of light-induced H motion<sup>23</sup> and H-mediated structural changes in  $\mu$ c-Si:H due to grain boundary motion,<sup>24</sup> it is possible that such hydrogenated interfacial regions are unstable under light soaking and thermal annealing, due to the catalytic function of locally mobile H in rearranging the local Si network structure. We can then describe the creation, saturation, and annealing processes of the light-induced metastable changes as follows.

A significant fraction of the energy deposited by carrier recombination may drive the local motion of H atoms,<sup>23</sup> so that the local bonding configurations may fluctuate, leading to fluctuations in the positions of the interfaces. The differential of local order across an interface situated between high- and low-ordered phases will entropically favor its motion into the more ordered phase, corresponding to the growth of the less ordered phase, and the increase in overall structural disorder and entropy. Indeed, light-induced reversible change of structural ordering in *a*-Si:H has been reported.<sup>25</sup> Furthermore, H flipping defects<sup>7</sup> could occur and provide a significant means for the local motion of H at the interfaces. However, these mechanisms alone should not create DB defects. Besides the increase in structural disorder, another driving force for structural change is the minimization of lattice strain energy. The tendency of the network to minimize the strain per bond by propagation to the rest of the network causes the growth of the less ordered phase to be imperfect, and leads to the creation of coordination defects (metastable DB's) that occur in conjunction with the phase growth. This two-phase picture is consistent with the weak-bond breaking model,<sup>3</sup> and suggests a spatial location of the weak bond, i.e., in the vicinity of the interfaces.

The strain initially concentrated at the interfaces is spread to the rest of the network as the growth of the less ordered phase proceeds, so that the interfaces gradually become less strained and stabilize, eventually leading to the end of the phase-growth process. Under the conditions of thermal annealing, the energy is made available to all the atoms, and the regrowth of the more ordered phase will be favored to satisfy local minimization of atomic configuration energy. This process, obtained by annealing at a suitable temperature, effectively reverses the phase growth induced by light soaking, metastable DB's are annihilated as the strain is re-concentrated at the interfaces and the material approaches a structural state similar to, but not necessarily the same as, the initial state.

The above phenomenological description of the metastability can be reconciled with the experimental results outlined above. The improved electronic stability of the H-diluted GD and the HW films is likely due to the predominance of Si-H (i.e., no Si-H<sub>2</sub>), and better overall network ordering. Proton NMR finds more clustered H, suggesting



more metastable interfaces, in the nondiluted film, and the DIR results suggest that Si-H<sub>2</sub> may lead to an extra metastability. The observation that the IR absorption coefficient exhibits metastable changes on the order of 1% is consistent with a picture in which at least a few percent of the H atoms are involved in bonding rearrangements related to the metastable phase-growth process. The lack of full recovery of the metastable changes indicates that the annealed structural state is not exactly the same as the initial state A, which is suggested by the model described here. A metastable increase in compressive stress would accompany the increase in volume fraction of the less ordered, less dense region, as well as the spreading of the strain initially concentrated at the interfaces to the rest of the network. The HW films are evidently much more inhomogeneous than the GD films, suggesting a larger fraction of interfacial regions in the HW *a*-Si:H. Thus, even though the HW film has much lower H content, a greater fraction of its H is likely to be associated with the metastable interfacial regions than that of the GD material. This is supported by the NMR observation that the H clusters contain a much larger number (>14 atoms) of H atoms in HW *a*-Si:H than that (six atoms) in GD *a*-Si:H.<sup>12</sup> Therefore, given the more inhomogeneous microstructure of the HW film, the model suggests that the magnitude of its light-induced structural changes should be larger than expectations based solely on H content, in agreement with the LOB and DIR data. Indeed, the photoinduced stress in the HW films decreases by only a factor of 2 over a range of H content that changes by a factor ~8.

This model can also explain several important observations.<sup>26–29</sup>

(1) The SWE has low efficiency; i.e., more than 10<sup>22</sup> cm<sup>-3</sup> recombination processes are needed for 10<sup>17</sup> cm<sup>-3</sup> new defects.<sup>26</sup> As described in the model, this is because (a) a large fraction of the recombination energy drives the structural changes, and (b) the defect creation does not take place uniformly in the whole *a*-Si:H network, but more likely takes place in the vicinity of the interfacial region.

(2) The order of magnitude increase in defect creation rate obtained with short, intense laser pulses,<sup>27</sup> is consistent with recombination-driven structural changes. The large recombination densities raise the effective “temperature” of the lo-

cally mobile H at the interfaces, increasing the phase-growth rate superlinearly with carrier density, and also increasing the effective number of metastable interfaces. The significant increase in saturated defect density excludes the possibility that a finite number of defect centers cause saturation, also consistent with the model. One would expect larger effects in DIR and LOB measurements by using such pulsed excitations.

(3) Time-resolved measurements of the electronic metastability of *a*-Si:H find that there is a slow precursor to defect creation with a time scale on the order of milliseconds, rather than the recombination time scale of microseconds.<sup>28</sup> The structural changes suggested in this model may correspond to that precursor.

(4) Further evidence for a two-phase *a*-Si:H microstructure is that when the H dilution ratio is increased in the CVD process, the highly ordered *a*-Si regions tend to crystallize into grains.<sup>9,29</sup>

In summary, the light-induced metastability of *a*-Si:H contains structural changes in conjunction with metastable DB creation. We describe the light-induced metastability by a two-phase amorphous model. We emphasize that both the reduced H clusters and the improved overall structural ordering are crucial for the improved stability. The high-H-diluted GD films grown just before the onset of microcrystallinity have shown improved stability as good as that of a HW film.<sup>30</sup> No simple correlation was observed between the light-induced structural changes and PC degradation, which does not obey a stretched-exponential rule. The inhomogeneity of the amorphous silicon network might be important in explaining the above results.

#### ACKNOWLEDGMENTS

D.H., J.B., and G.Y. are supported by the NREL. Thin Film PV partnership, Sub-subcontract No. XAK-8-17619-11, and partially by NSF Grant Nos. INT-9604915 and INT-9600229. We are grateful for help with the DIR studies to G. Kong in Beijing, China, and with the stress studies to S. Nitta, S. Nonomura, and T. Gotoh in Gifu, Japan. The samples were made by the NREL *a*-Si group and Solarex thin film division.

<sup>1</sup>D. L. Staebler and C. R. Wronski, Appl. Phys. Lett. **31**, 292 (1977).

<sup>2</sup>H. Fritzsche, in *Amorphous and Microcrystalline Silicon Technology—1997*, MRS Symposia Proceedings No. 467, edited by S. Wagner, M. Hack, E. A. Schiff, R. Schropp, and I. Shimizu (Materials Research Society, Pittsburgh, 1997), p. 19.

<sup>3</sup>M. Stutzmann, W. B. Jackson, and C. C. Tsai, Phys. Rev. B **32**, 23 (1985).

<sup>4</sup>H. M. Branz, Sally Asher, H. Gleskova and S. Wagner, Phys. Rev. B **59**, 5513 (1999).

<sup>5</sup>Yiping Zhao, Guanglin Kong, Guangqin Pan, and Xianbo Liao, Phys. Rev. Lett. **74**, 558 (1995).

<sup>6</sup>T. Gotoh, S. Nonomura, M. Nishio, S. Nitta, M. Kondo, and A. Matsuda, Appl. Phys. Lett. **72**, 2978 (1998).

<sup>7</sup>R. Biswas and Y. P. Li, Phys. Rev. Lett. **82**, 2512 (1999).

<sup>8</sup>A. H. Mahan, J. Carapella, B. P. Nelson, R. S. Crandall, and I. Balberg, J. Appl. Phys. **69**, 6728 (1991).

<sup>9</sup>D. V. Tsu, B. S. Chao, S. R. Ovshinsky, S. Guha, and J. Yang, Appl. Phys. Lett. **71**, 1317 (1997).

<sup>10</sup>L. Yang and L. Chen, Appl. Phys. Lett. **63**, 400 (1993).

<sup>11</sup>Daxing Han, Keda Wang, and Liyou Yang, J. Appl. Phys. **80**, 2475 (1996).

<sup>12</sup>Y. Wu, J. T. Stephen, Daxing Han, J. M. Rutland, R. S. Crandall, and A. H. Mahan, Phys. Rev. Lett. **77**, 2049 (1996).

<sup>13</sup>Xiao Liu, B. E. White, Jr., R. O. Pohl, E. Iwanizcko, K. M. Jones, A. H. Mahan, B. P. Nelson, R. S. Crandall, and S. Veprek, Phys. Rev. Lett. **78**, 4418 (1997).

<sup>14</sup>We note that HW films deposited at ~350 °C were found to contain ~90% of their H in the clustered phase (Ref. 12). In this work, the HW film was prepared at a substrate temperature of

- 410 °C, so it is reasonable that the clustered H is reduced to ~70%.
- <sup>15</sup>J. Baugh, Daxing Han, A. Kleinhammes, Q. Wang, and Y. Wu (unpublished).
- <sup>16</sup>Daxing Han, Guozhen Yue, Jing Lin, H. Habuchi, Eugene Iwaniczko, and Qi Wang, in *Amorphous and Heterogeneous Silicon Thin Films: Fundamental to Devices*, MRS Symposia Proceedings (Materials Research Society, Pittsburgh, in press).
- <sup>17</sup>Jackson and Amer, Phys. Rev. B **25**, 5559 (1982).
- <sup>18</sup>Daxing Han and H. Fritzsche, J. Non-Cryst. Solids **59/60**, 397 (1983).
- <sup>19</sup>R. A. Street, *Hydrogenated Amorphous Silicon* (Cambridge University Press, Cambridge, 1991).
- <sup>20</sup>Benyuan Gu, Daxing Han, Chenxi Li, and Shifu Zhao, Philos. Mag. B **53**, 321 (1986).
- <sup>21</sup>L. Jiao, H. Liu, S. Semoushikina, Y. Lee, and C. R. Wronski, Appl. Phys. Lett. **69**, 3713 (1996).
- <sup>22</sup>H. M. Branz and M. Silver, Phys. Rev. B **42**, 7420 (1990).
- <sup>23</sup>H. M. Branz, S. E. Asher, and B. P. Nelson, Phys. Rev. B **47**, 7061 (1993).
- <sup>24</sup>I. Kaiser, N. H. Nickel, W. Fuhs, and W. Pilz, Phys. Rev. B **58**, R1718 (1998).
- <sup>25</sup>Daxing Han, Changhua Qiu, and Wenhao Wu, Philos. Mag. B **54**, L9 (1986). A light-induced change of the slope of the optical absorption edge was observed parallel with the increase of sub-band-gap absorption, and has been explained by an increase of structure disorder.
- <sup>26</sup>H. Fritzsche, J. Non-Cryst. Solids **59/60**, 1289 (1983).
- <sup>27</sup>M. Stutzmann, J. Nunnenkamp, M. S. Brandt, and A. Asano, Phys. Rev. Lett. **67**, 2347 (1991).
- <sup>28</sup>H. M. Branz, Phys. Rev. B **59**, 5498 (1999).
- <sup>29</sup>Guozhen Yue, J. D. Lorentzen, Jing Lin, Qi Wang, and Daxing Han, Appl. Phys. Lett. **75**, 492 (1999).
- <sup>30</sup>S. Guha, J. Yang, D. L. Williamson, Y. Lubianiker, J. D. Cohen, and A. H. Mahan, Appl. Phys. Lett. **74**, 1860 (1999).